Validation of Pedestrian Lower Limb Injury Assessment using Subsystem Impactors

Yukou Takahashi[1], Miwako Ikeda[1], Iwao Imaizumi[1], Yuji Kikuchi[1], Satoru Takeishi[1]

Abstract Although the biofidelity improvements of the pedestrian legform called the Flexible Pedestrian Legform Impactor (FlexPLI) relative to the conventional legform (EEVC legform) have been shown in past studies, their effects on the evaluation of safety performance of vehicles have not been clarified in a quantitative and comprehensive manner. The goal of this study was to clarify the difference in the results of the tibia and knee injury assessment between the two legforms, and the factors of the difference from a viewpoint of their stiffness characteristics and injury measures. Impact simulations were conducted at 40 km/h using the finite element (FE) models of the two legforms and a human body, along with 18 simplified vehicle models. The correlation between the peak tibia and knee injury measures from the human model and those from the two legform models showed significant improvements of the FlexPLI for tibia fracture and ACL failure prediction. Additional impact simulations using simplified vehicle models showed that both the stiffness of the tibia and the use of the acceleration as an injury measure are the factors for the poor correlation of tibia injury measures of the EEVC legform.

Keywords Human FE Model, Injuries, Tibia and Knee, Legforms, Pedestrians

I. INTRODUCTION

Due to a significant percentage of pedestrians in traffic fatalities, pedestrian protection has been attracting a great social attention worldwide. According to the International Road Traffic and Accident Database (IRTAD) established by the OECD Road Transport Research Programme, pedestrian fatalities account for 12.1% in US, 11.6% in France, 14.2% in Germany, 22.4% in UK, 32.1% in Poland, 34.9% in Japan, and 36.6% in Korea of all traffic fatalities in year 2009 [1]. Japanese [2] and US [3] accident databases show that the lower limb is the most frequently injured body region in pedestrian serious injuries. In order to address pedestrian lower limb injuries, the subsystem test procedure developed by the European Enhanced Vehicle-safety Committee (EEVC) has been widely used in regulations and new car assessment programs. In this test procedure, the legform impactor developed by the Transport Research Laboratory (EEVC legform) is used. Although the test procedure was incorporated into the United Nations Global Technical Regulation on pedestrian safety (UN GTR No.9) [4] adopted by the World Forum for Harmonization of Vehicle Regulations (WP.29) under the UN, the improvement of the EEVC legform has been an issue in terms of both biofidelity and repeatability.

In order to improve the biofidelity of the conventional EEVC legform for further mitigation of pedestrian serious injuries, Japan Automobile Manufacturers Association (JAMA) and Japan Automobile Research Institute (JARI) have jointly developed the Flexible Pedestrian Legform Impactor (FlexPLI) [5]. The biofidelity improvements of the FlexPLI relative to the EEVC legform have been clarified in past studies. In terms of the biofidelity of the conventional EEVC legform, Matsui et al. [6] compared the time histories of the impact force, knee shearing displacement and knee bending angle against published experiments in knee bending and shearing test setups using Post Mortem Human Subjects (PMHSs) performed by Kajzer et al., showing that the EEVC legform does not have sufficient biofidelity. In addition, Konosu et al. [7] performed impact simulations using an EEVC legform model and a human finite element (FE) model along with 18 simplified car models with various front end geometry and stiffness, and found that there is no correlation (R=0.01) between the human tibia bending moment and the EEVC legform upper tibia acceleration. The biofidelity of the second latest version of the FlexPLI (FlexPLI Type GT) was evaluated by Konosu et al. [8] using a similar methodology to that employed

Yukou Takahashi is Chief Engineer (e-mail: yukou_takahashi@n.t.rd.honda.co.jp), Miwako Ikeda is Engineer (e-mail: miwako_ikeda@n.t.rd.honda.co.jp), Iwao Imaizumi is Assistant Chief Engineer (e-mail: iwao_imaizumi@n.t.rd.honda.co.jp), Yuji Kikuchi is

by their knee study [7]. Impact simulations against 18 simplified vehicle models were performed using an FE model of the FlexPLI Type GT and a human FE model. The results showed that the correlation of the human model and FlexPLI model tibia bending moments was much better (R=0.90) than the correlation between the human model tibia bending moment and the EEVC legform upper tibia acceleration (R=0.01). In addition, similar computational study done by JAMA and JARI [9] revealed that the correlation of the tibia bending moment between an FE model of the latest version of the FlexPLI (FlexPLI Type GTR; hereafter called FlexGTR) and a human FE model was as good as that of the FlexPLI Type GT (R=0.90). These studies have indirectly shown significant biofidelity improvements of the FlexPLI relative to the EEVC legform particularly with regard to tibia fracture measures. Although some of these studies used the bending moment as a predictor of human tibia fracture, the validity of the use of the bending moment has not been clarified. No comparison has been made as to the correlation of all the injury measures in car impacts between a human body and the two legforms. In addition, the factors for the difference in the correlation have not been clarified.

The goal of this study was to clarify the difference between the FlexGTR and the EEVC legform in the correlation of the tibia and knee injury measures with a human body, and the factors of the difference from a viewpoint of the tibia stiffness characteristics and the injury measures used. Impact simulations against simplified vehicle models were conducted using a human FE model to identify the best predictor of tibia fracture. Similar impact simulations were also performed using FE models of both legforms to evaluate the correlation of the peak tibia and knee injury measures from the two legform models with those from the human model. The results of the correlation analysis showed that the correlation with the human response was much better with the FlexGTR for the tibia fracture and ACL failure measures. In addition, the correlation between the EEVC legform upper tibia acceleration and the human model tibia bending moment showed a negative correlation between them. In order to further investigate the factors for the poor correlation of the upper tibia acceleration of the EEVC legform, additional simulations were conducted using simplified vehicle models with the bumper location and stiffness individually varied.

II. METHODS

Predictor of Tibia Fracture

The EEVC legform and the FlexGTR use the upper tibia acceleration and the tibia bending moment, respectively, as injury measures for tibia fracture. Since these two measures are essentially different, the predictor that best describes pedestrian tibia fracture was investigated to determine the physical parameter to be used when correlating human and impactor responses.

In order to cover a variety of vehicle front end structure and stiffness characteristics, 18 simplified vehicle models used by Konosu et al. [7][8] were also used in this study. Figures 1 and 2 respectively show the schematic of the structure of the simplified vehicle models, and the definition of geometric parameters used to represent the variation among vehicles. The bonnet leading edge (BLE) was modeled using deformable shell elements representing a sheet metal structure, while the bumper (BP) and the spoiler (SP) were modeled as rigid bodies. BP, SP and the lateral ends of BLE were connected via joint elements with springs to a node with the mass of 1500 kg that represented the mass of the vehicle. The stiffness characteristics were specified by the thickness of the shell elements and the joint characteristics for BLE and BP/SP, respectively. Figure 3 shows the stiffness characteristics used for BP and SP. Table I summarizes the levels of the geometric and stiffness parameters varied among the models. Three different levels were used except BLE thickness that was classified into two levels. 18 different combinations of the geometric and stiffness parameters were determined using L18 orthogonal array to develop vehicle models that can be used to investigate the effect of each parameter with a minimal number of models. Table II summarizes the combinations of the parameters specified in the 18 models. More details of the simplified vehicle models are given by Konosu et al. [7][8].

Assistant Chief Engineer (e-mail: yuuji_kikuchi@n.t.rd.honda.co.jp), Satoru Takeishi is Assistant Chief Engineer (e-mail: satoru_takeishi@n.t.rd.honda.co.jp), all at Honda R&D Co., Ltd. Automobile R&D Center in Japan (tel: +81-28-677-3311).

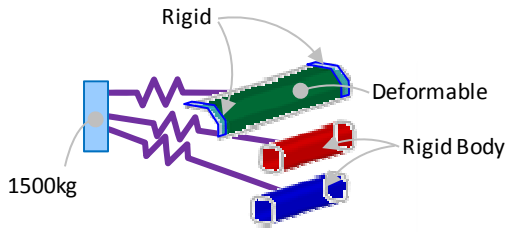

Fig. 1. Schematic of simplified vehicle model

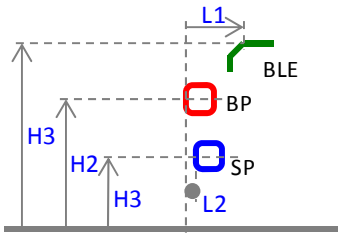

Fig. 2. Definition of geometric parameters

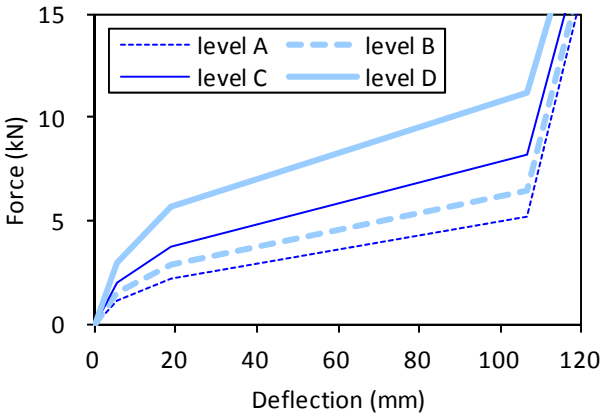

Fig. 3. Stiffness characteristics used for BP and SP

TABLE I
LEVELS OF GEOMETRIC AND STIFFNESS PARAMETERS

Parameter	Unit	Level 1	Level 2	Level 3
K1 (BLE stiffness)	mm	0.4	0.6	
K2 (BP stiffness)	-	B	C	D
K3 (SP stiffness)	-	A	C	D
H1 (BLE height)	mm	650	700	750
H2 (BP height)	mm	450	490	530
H3 (SP height)	mm	250	270	350
L1 (BLE lead)	mm	125	200	275
L2 (BLE lead)	mm	-20	0	30

TABLE II
COMBINATIONS OF GEOMETRIC AND STIFFNESS PARAMETERS

ID	K1	K2	K3	H1	H2	H3	L1	L2	ID	K1	K2	K3	H1	H2	H3	L1	L2
S1	0.4	B	A	650	450	250	125	-20	S10	0.6	B	A	750	530	270	200	-20
S2	0.4	B	C	700	490	270	200	0	S11	0.6	B	C	650	450	350	275	0
S3	0.4	B	D	750	530	350	275	30	S12	0.6	B	D	700	490	250	125	30
S4	0.4	C	A	650	490	270	275	30	S13	0.6	C	A	700	530	250	275	0
S5	0.4	C	C	700	530	350	125	-20	S14	0.6	C	C	750	450	270	125	30
S6	0.4	C	D	750	450	250	200	0	S15	0.6	C	D	650	490	350	200	-20
S7	0.4	D	A	700	450	350	200	30	S16	0.6	D	A	750	490	350	125	0
S8	0.4	D	C	750	490	250	275	-20	S17	0.6	D	C	650	530	250	200	30
S9	0.4	D	D	650	530	270	125	0	S18	0.6	D	D	700	450	270	275	-20

The 18 simplified vehicle models were made to collide with a human body model laterally from the left at 40 km/h. The human body model developed by the authors in their previous studies [10][11] was used. Figure 4 shows the schematics of the human model. The pelvis and the lower limb were modeled using shell and solid elements to accurately represent geometric and material characteristics of these body regions. Quasi-static and dynamic response and failure characteristics of the pelvis and lower limb models were extensively validated against published experiments. The model validations included lateral compression of the pelvis in acetabulum and iliac loadings, 3-point bending of the thigh, femur, leg, tibia and fibula at multiple loading locations, tension of the individual knee ligament and 4-point bending of an isolated knee joint. The upper part of the body was modeled using articulated rigid bodies with all of the seven cervical and five lumbar vertebrae individually modeled to represent flexibility of these regions. The full-body pedestrian model was validated against published full-scale car-pedestrian impact experiments in terms of trajectories of the head, top and middle of the thorax, and the pelvis, along with pelvis and lower limb injury prediction in collisions with a small sedan and a large SUV. Figure 5 illustrates the model setup. The left lower limb was in a vertical position and the right lower limb was rotated about the hip joint anteriorly by 20 degrees. This posture was chosen to compare the results of the human model with those of the legform models that are supposed to collide with the vehicle in an upright position. In this position, the leg is primarily subjected to bending moment, shear force and tensile force during the loading from the bumper. Assuming that bone fails when the local bone stress (von Mises stress)

exceeds the limit, the correlation between the peak local bone stress and the values of these measures at the time of peak von Mises stress was investigated to identify the best predictor of tibia fracture. Section force and moment were used to determine the peak values of the bending moment, shear force and tensile force. Since the FlexGTR measures the tibia bending moment at four locations, the cross-sections in the tibia of the human model corresponding to the FlexGTR measurement locations were determined. For each impact simulation, the cross-section generating the maximum local bone stress was used for the correlation analysis. Since the EEVC legform evaluates the upper tibia acceleration (acceleration of the tibia 66 mm below the knee joint), the correlation was also investigated between the peak local bone stress and the acceleration of the tibia at the corresponding location (node nearest to the accelerometer location) of the human model.

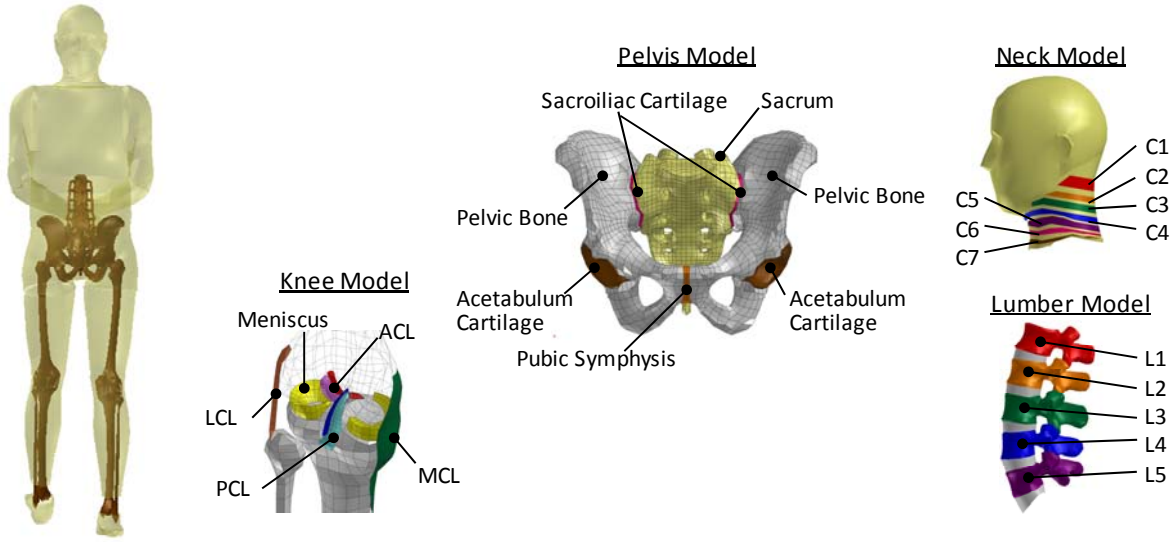

Fig. 4. Human FE model

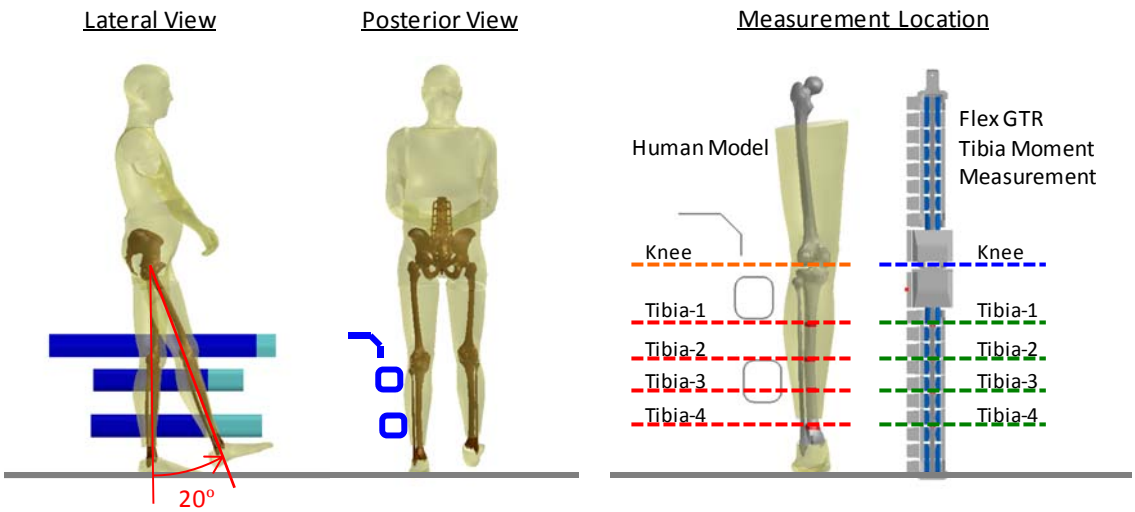

Fig. 5. Human model setup

Development and Validation of Legform Models

Figure 6 shows the structure and instrumentation of the EEVC legform, along with the schematics of the FE model of the EEVC legform. The femur and tibia shafts consist of a steel tube and are virtually rigid. The deformation of the steel plates at the knee joint simulates knee bending. Knee shearing is provided by the motion of the cantilever installed in the femur shaft. The knee shear displacement and the knee bending angle are used as measures for the failure of the Medial Collateral Ligament (MCL) and the Anterior Cruciate Ligament (ACL), respectively. The upper tibia acceleration measured by the accelerometer installed below the knee joint is used as a tibia fracture measure. The femur and tibia shafts of the legform were modeled as rigid bodies, surrounded by a foam material modeled using solid elements. The cantilever was modeled using shell elements with the top end rigidly connected to the femur shaft. The bottom end of the cantilever was connected to a

node, which was connected to the femur shaft via a spring element with damping characteristics. The node and the tibia shaft were connected by a joint element with bending characteristics. The model validation included the quasi-static knee bending and shearing certification tests and the dynamic certification test as specified in the UN GTR No.9 [4], along with three vehicle tests, as summarized in Table III. The vehicle tests were performed at 40 km/h with the impact location being the center of the vehicle laterally. Three vehicles representing a passenger car, a sport car and an SUV were used.

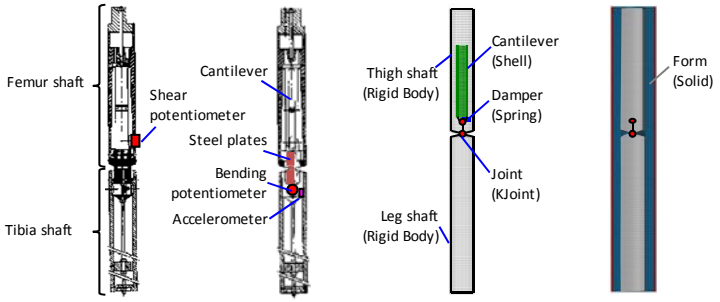

Fig. 6. Structure and instrumentation of EEVC legform and schematics of EEVC legform model

TABLE III
EEVC LEGFORM MODEL VALIDATION

Component	Assembly
• Quasi-static knee bending • Quasi-static knee shearing	• Dynamic certification test • Vehicle test

Figure 7 shows the structure and instrumentation of the FlexGTR, along with the schematics of the FE model of the FlexGTR. The femur and tibia shafts consist of the flexible bone core made of glass fiber reinforced vinyl ester resin, the core binder, the exterior housing and the rubber buffer. The bending characteristics of the human femur and tibia are represented primarily by the bone core. Four major knee ligaments (MCL, ACL, PCL (Posterior Cruciate Ligament) and LCL (Lateral Collateral Ligament)) are represented by wire cables with springs on both femur and tibia sides that provide tensile stiffness of the ligaments. The strain gages affixed to the tibia bone core in four different cross-sections measure the bending moment used as the tibia fracture measure. Failure of the MCL, ACL and PCL are evaluated by measuring the ligament elongation using potentiometers. The entire legform is surrounded by the Neoprene with a rubber layer inside. In the FE model of the FlexGTR, the bone cores, Neoprene and the rubber layer were modeled using deformable solid elements, while the core binder and exterior housing were modeled as rigid bodies. The ligament cables were modeled using bar elements that represent the compressive characteristics of the springs on both sides of the cable. The model validation included quasi-static 3-point bending of the bone core, femur, knee and tibia, assembly pendulum test, and simplified and actual vehicle impact tests, as summarized in Table IV. The 3-point bending bone core certification tests are specified in the FlexPLI Technical Evaluation Group (Flex-TEG) document [12]. The 3-point bending femur, knee and tibia certification tests and the pendulum certification tests are specified in the proposal for amendment 2 of UN GTR No.9 [13].

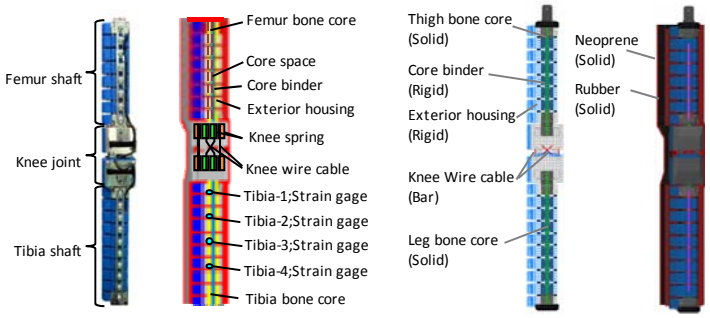

Fig. 7. Structure and instrumentation of FlexGTR and schematics of FlexGTR model

TABLE IV
FlexGTR MODEL VALIDATION

Component	Assembly
• Quasi-static 3-point bending of bone core • 3-point bending of femur • 3-point bending of knee • 3-point bending of tibia	• Pendulum test • Simplified car test • Vehicle test

Correlation of Injury Measures between Human and Legform Models

The two legform models were subjected to lateral impact from the 18 simplified vehicle models at 40 km/h. The TRL legform model and the FlexGTR model were set up in accordance with the test procedures specified in the UN GTR No.9 [4] and the proposal for amendment 2 of UN GTR No.9 [13], respectively. The correlation

between the peak values from the human model and the legform models was investigated for the injury measures of three types of injury – tibia fracture, MCL failure and ACL failure. For the tibia fracture, the tibia bending moment of the human model was used because the measure was identified as the best predictor of tibia fracture in car-pedestrian collisions. Based on the mechanical function of the knee ligaments, the elongation of the MCL and the ACL were used for the human model. The injury measures used with the two legforms were also used in this correlation analysis (EEVC legform model: upper tibia acceleration, knee bending angle and knee shear displacement; FlexGTR model: tibia bending moment, MCL elongation and ACL elongation, as the injury measures for the tibia fracture, MCL failure and ACL failure, respectively).

Factors for Difference in Tibia Fracture Measure Correlation

The factors determining the correlation of the tibia fracture measures were further investigated by running some additional impact simulations. In order to investigate the individual effect of the stiffness and geometric characteristics of a vehicle, a baseline simplified vehicle model was set up. Based on the model S1 in Table II, the SP lead (L2) was changed to 30 mm and the BP stiffness was changed from level B to level D, both to clearly show the effect of the bumper stiffness change. The BLE lead (L1) was switched to 275 mm to minimize the contribution from the bonnet leading edge to the tibia response. Relative to the baseline model, the stiffness characteristics of BP and SP were individually changed to represent bottoming of these components as shown in Figure 8. Relative to the case with a stiff SP, the horizontal location of SP was changed as illustrated in Figure 9. In order to investigate the effect of the tibia stiffness, the rigid body tibia of the EEVC legform model was switched to deformable, and the elastic modulus for steel (Tibia Stiffness = Steel) and the elastic modulus that approximates the flexural rigidity of the human tibia (555.6 Nm^2) (Tibia Stiffness = Bone) were applied to the shell elements comprising the tibia of the EEVC legform model. Table V summarizes the cases of the impact simulations performed. As a result of the combination of the vehicle characteristics and the tibia stiffness, 10 impact simulations were performed.

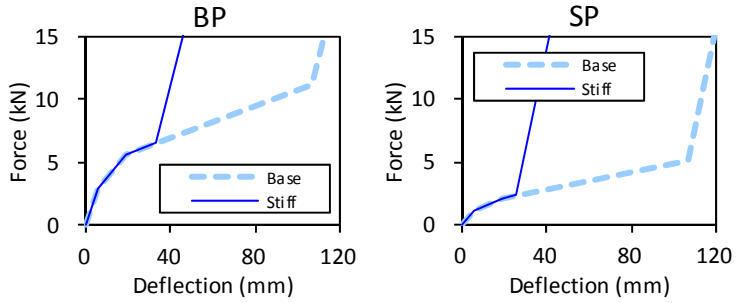

Fig. 8. Stiffness characteristics of BP and SP

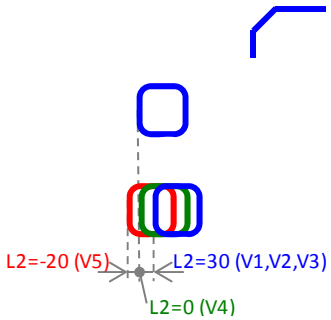

Fig. 9. SP locations

TABLE V
IMPACT SIMULATION CASES

Case	BP Stiffness	SP Stiffness	SP Location (L2 in mm)	Tibia Stiffness	Case	BP Stiffness	SP Stiffness	SP Location (L2 in mm)	Tibia Stiffness
V1-B	Base	Base	30	Bone	V1-S	Base	Base	30	Steel
V2-B	Stiff	Base	30	Bone	V2-S	Stiff	Base	30	Steel
V3-B	Base	Stiff	30	Bone	V3-S	Base	Stiff	30	Steel
V4-B	Base	Stiff	0	Bone	V4-S	Base	Stiff	0	Steel
V5-B	Base	Stiff	-20	Bone	V5-S	Base	Stiff	-20	Steel

One of the findings from the impact simulations above was that the change of the peak values showed an opposite trend between the tibia bending moment and the tibia acceleration, when SP location was changed. In order to give clarifications to the sensitivity of both measures to the magnitude and the location of the applied load, some additional impact simulations were performed using the tibia (without flesh) of the EEVC legform model used above (Tibia Stiffness = Bone) along with a single impactor. Figure 10 shows the leg impact simulation setup. The height of the impactor was set at 20 mm with a half-cylindrical tip. The impactor was modeled as a rigid body and was connected to a node with the mass of 1500 kg via a spring element. The ramp

and hold functions shown in Figure 11 were applied to the force-deflection characteristics of the spring element to provide two different levels of the impact force. The tibia model consisted of shell elements with a thickness of 10 mm. The elastic modulus of 637.3 MPa was used to simulate the flexural rigidity of the human tibia. The vertical dimension of the tibia model was slightly modified to 500 mm from the tibia model of the EEVC legform for simplification. The mass of the tibia model was set at 3.9 kg to represent the mass of the tibia of the EEVC legform. Three impact heights were used to investigate the effect of the impact location relative to the center of gravity (CG) of the tibia model. The single impactor was made to collide with the tibia model at 40 km/h. Table VI summarizes the simplified tibia impact simulation cases.

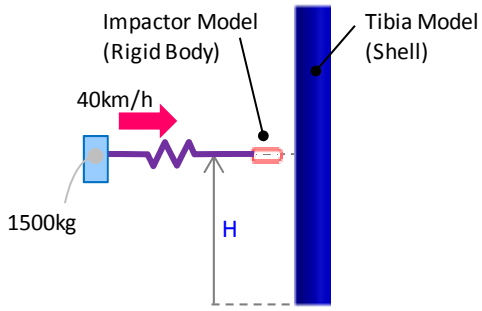

Fig. 10. Simplified tibia impact simulation setup

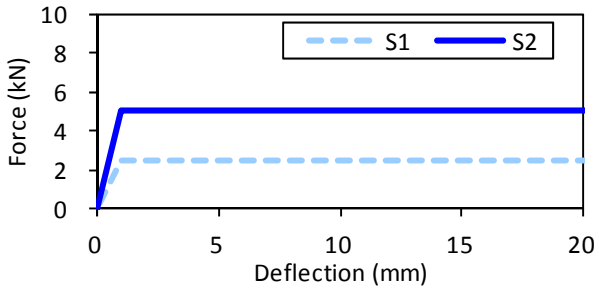

Fig. 11. Stiffness characteristics of impactor

TABLE VI
SIMPLIFIED TIBIA IMPACT SIMULATION CASES

Case	Impact Height (H in mm)	Impactor Stiffness (Force level in kN)	Case	Impact Height (H in mm)	Impactor Stiffness (Force level in kN)
H1-S1	250	2.5	H1-S2	250	5.0
H2-S1	350	2.5	H2-S2	350	5.0
H3-S1	450	2.5	H3-S2	450	5.0

III. RESULTS

Predictor of Tibia Fracture

Figure 12 shows the correlation between the peak von Mises stress and the peak values of the bending moment, upper tibia acceleration, shear force and tensile force, respectively, at the time of peak von Mises stress from the human FE model. The correlation coefficient was by far the largest for the bending moment (R=0.79) than the other three measures, showing that the bending moment is the best predictor among these four measures. The tensile force and the shear force exhibited a much larger scatter compared to the bending moment. Two thirds of the data points from the upper tibia acceleration showed a "flat" distribution, with the rest of one third of the data points showing a very large deviation from the other group. Based on the results, the following correlation analysis used the tibia bending moment as a predictor of tibia fracture in car-pedestrian collisions.

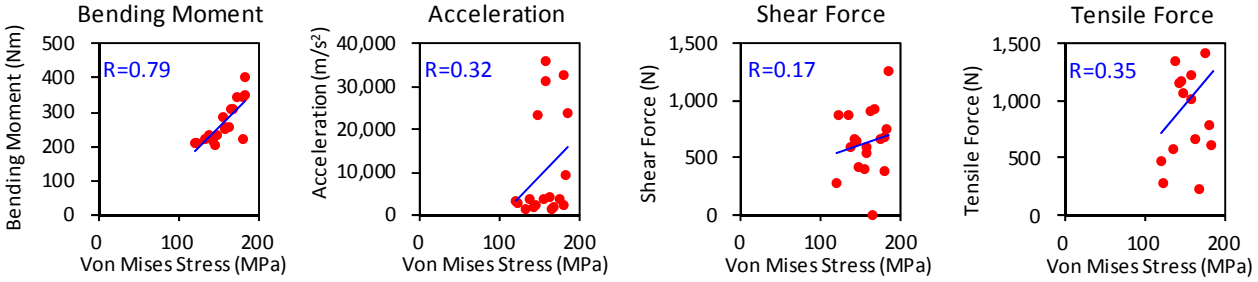

Fig. 12. Correlation between peak von Mises stress and peak values of bending moment, upper tibia acceleration, shear force and tensile force at time of peak von Mises stress

Development and Validation of Legform Models

In terms of the validation results for the EEVC legform model, the force-angle and force-shearing displacement response in quasi-static knee bending and shearing test predicted by the model fell within the corridors specified in the UN GTR No.9 [4] for the bending and shearing certification tests, respectively. The predicted peak upper tibia acceleration, knee bending angle and knee shearing displacement in the dynamic certification test all fell within the range specified in the UN GTR No.9 as a requirement. Figure 13 shows the results of the model validation in the vehicle impact tests using a passenger car, a sport car and an SUV. The peak knee bending angle and upper tibia acceleration predicted by the model well represented the difference between the vehicles and fell within ± 15% of the test results.

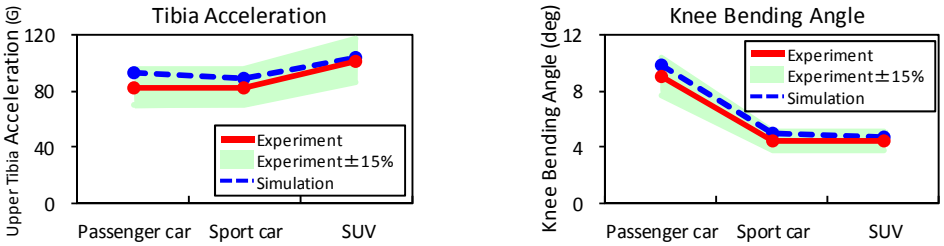

Fig. 13. EEVC legform model validation results in vehicle impact

With regard to the FlexGTR model, the predicted moment-deflection curves from the 3-point bending tests of the femur and tibia bone cores fell within the requirement corridors specified in the Flex-TEG document [12]. The moment-deflection curves from the 3-point bending of the femur and tibia, as well as the moment-elongation curve of the MCL and the elongation-force curves of the ACL and PCL from the 3-point bending of the knee, all fell within the corridor requirements specified in the proposal for amendment 2 of UN GTR No.9 [13]. In the pendulum certification tests, the predicted peak values of the four tibia bending moments and the elongations of the MCL, ACL and PCL all fell between the upper and lower limits specified in the proposal for amendment 2 of UN GTR No.9. In the simplified car impact test, the predicted peak values of all the injury measures were within ± 15% of the average of the three test results, except the PCL elongation (test average -15.8%). Figure 14 shows the results of the model validation against the vehicle impact tests using a passenger car, a sport car and an SUV. The peak values of the four tibia bending moments and the elongation of the ACL, PCL and MCL all fell within ± 15% of the test results for all of the three vehicles.

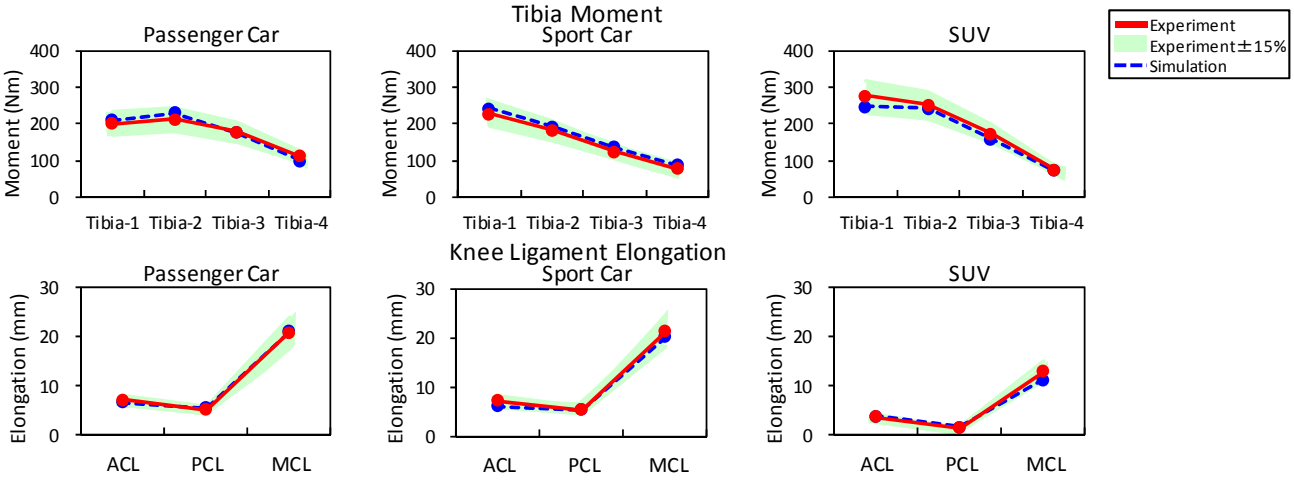

Fig. 14. FlexGTR model validation results in vehicle impact

Correlation of Injury Measures between Human and Legform Models

Figure 15 shows the correlation of the injury measures for the tibia fracture, MCL failure and ACL failure between the human model and the legform models. As for the tibia fracture measures, the upper tibia acceleration of the EEVC legform model showed a negative correlation with the tibia bending moment of the human model, with the correlation coefficient of 0.22. In contrast, the tibia bending moment of the FlexGTR

showed a much higher correlation (R=0.87). In terms of the MCL failure measures, the correlation with the human model MCL elongation was better for the knee bending angle of the EEVC legform model (R=0.75) than the MCL elongation of the FlexGTR model (R=0.56). With regard to the correlation with the ACL elongation of the human model, the knee shear displacement of the EEVC legform model exhibited no correlation (R=0.09), while the ACL elongation of the FlexGTR model showed a much better correlation (R=0.71).

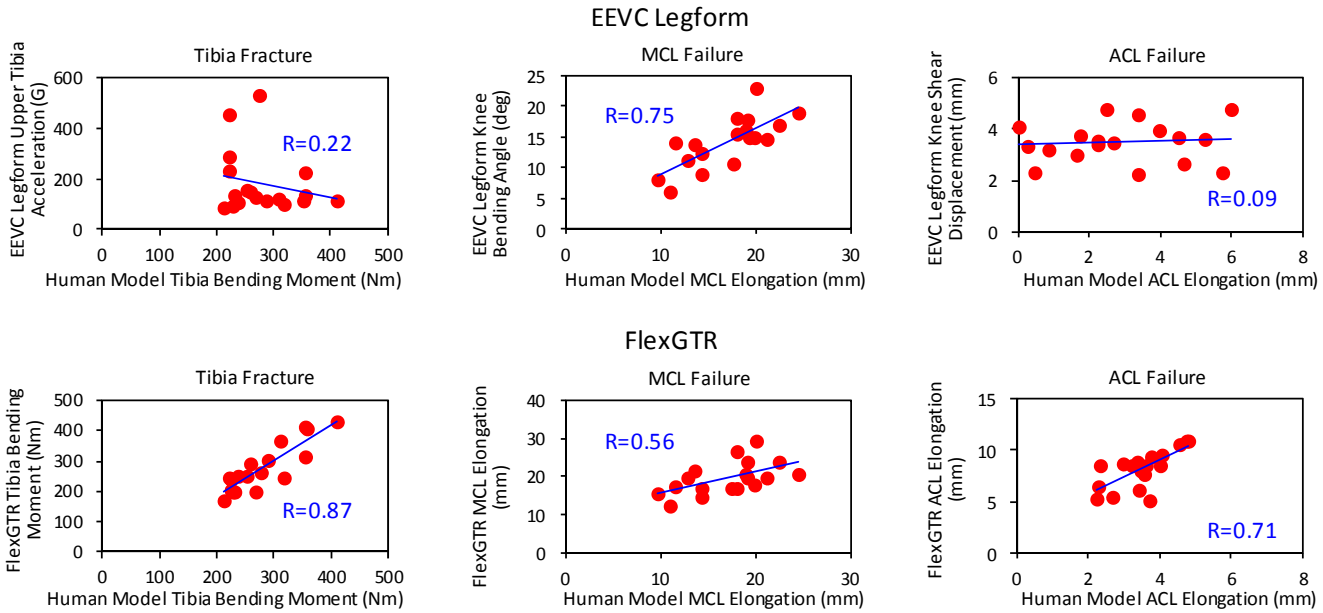

Fig. 15. Correlation of injury measures for tibia fracture, MCL failure and ACL failure between human model and legform models

Factors for Difference in Tibia Fracture Measure Correlation

Figures 16 and 17 illustrate the results of the peak tibia bending moment and the peak tibia acceleration. The peak values were taken at the heights of BP and SP. Figure 16 shows the change of the peak moment and the peak acceleration normalized by the results from the simplified vehicle model V1 (see Table V), when the stiffness of BP and SP were changed (vehicle model V1, V2 and V3). Figure 17 depicts the change of the peak moment and the peak acceleration normalized by the results from the simplified vehicle model V3, when SP location was varied (vehicle model V3, V4 and V5). The results for both tibia stiffness levels (Tibia Stiffness = Bone and Steel in Table V) are presented.

Overall, the results from Steel tibia stiffness exhibited larger change in the peak injury measures than those from Bone tibia stiffness. In Figure 16 showing the effect of BP and SP stiffness change, the bending moment and the acceleration at BP height showed a similar trend, while the acceleration was exceptionally high for the combination of Steel tibia stiffness and the vehicle model V2 (increased BP stiffness). In Figure 17, the trend of the change of the peak injury measures at BP height when SP location was varied was totally different between the bending moment and the acceleration. When SP location was moved forward from the vehicle model V3 to V5, the peak bending moment monotonically decreased, while the peak acceleration monotonically increased. The results at SP height showed a similar trend between the bending moment and the acceleration, except the acceleration for the combination of Steel tibia stiffness and the vehicle model V4.

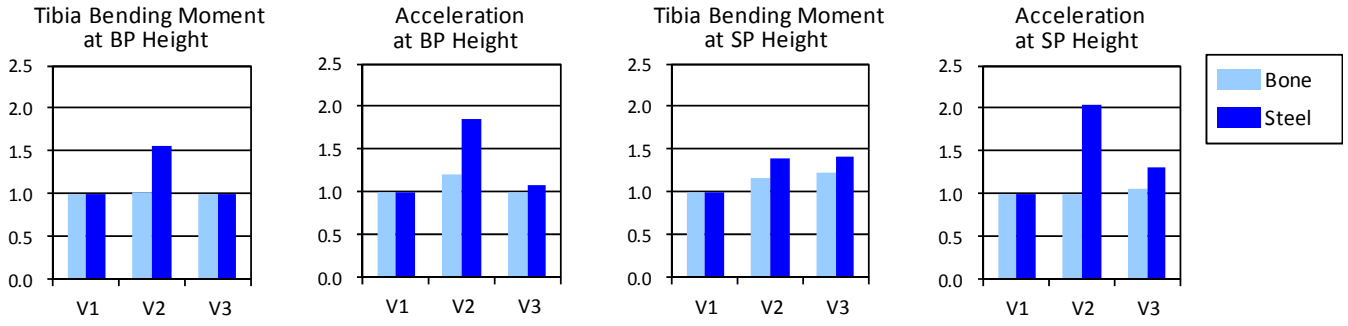

Fig. 16. Peak tibia bending moment and acceleration normalized by results from vehicle model V1 at BP and SP heights for vehicle models V1, V2 and V3

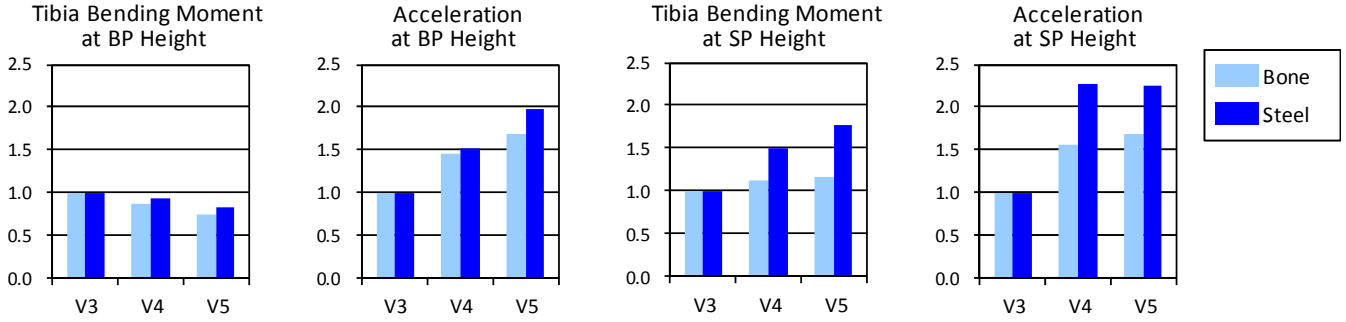

Fig. 17. Peak tibia bending moment and acceleration normalized by results from vehicle model V3 at BP and SP heights for vehicle models V3, V4 and V5

Figure 18 shows the results from the leg impact simulations. The peak values of the tibia bending moment and the tibia acceleration were taken at the height of the impactor. All the results were normalized by the results of case H1-S1 in Table VI. For each impactor height, both the bending moment and the acceleration were almost two times higher for the impactor stiffness S2 (5.0 kN) compared to S1 (2.5 kN). The acceleration was almost constant for the same impactor stiffness, regardless of the impactor height. In contrast, for both impactor stiffness levels, the bending moment decreased significantly as the impactor height increased.

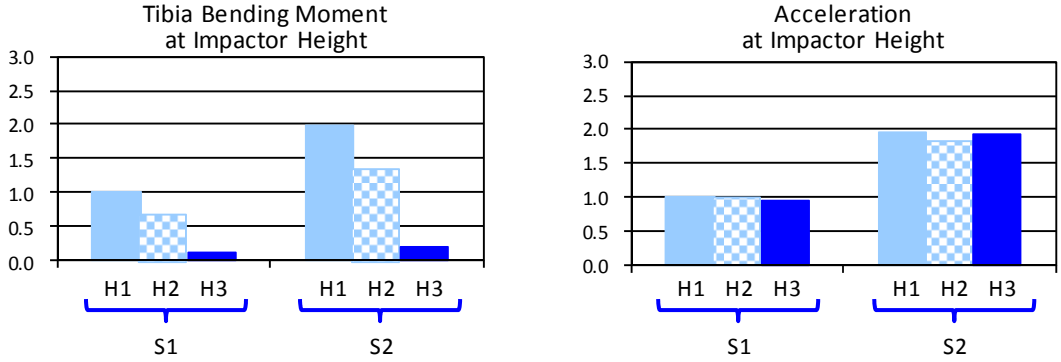

Fig. 18. Peak tibia bending moment and acceleration normalized by results from case H1-S1

IV. DISCUSSION

The results of the correlation analysis between the peak von Mises stress and the tibia fracture measures at the time of peak von Mises stress using the human FE model showed that the bending moment of the tibia best correlates with the stress. When a vehicle hits a pedestrian, the pedestrian body wraps around the vehicle front end. Due to this wrap around motion, the feet of the pedestrian come off the ground due to the rotation of the pedestrian body. Since the load applied to a pedestrian from a vehicle front end is primarily in a horizontal direction, the tensile force in the tibia is mainly generated by the inertial force during the wrap around motion, which is not determined solely by the applied load. In our previous study [14], a preliminary investigation showed that the peak injury measures normalized by the thresholds estimated from past studies were the highest for bending moment compared to shear and axial forces in impacts from all of the three vehicle types investigated. This suggests that the contribution from the shear force is smaller than that from the bending moment, resulting in a larger variability of the shear force in the correlation analysis.

The results of the correlation analysis of the injury measures between the human model and the two legform models showed that the correlation with the human model was significantly improved with the FlexGTR relative to the EEVC legform with regard to the tibia fracture and ACL failure measures. When the bumper hits the upper part of the tibia of a pedestrian, the struck-side knee joint is subjected to shear, followed by valgus bending due to the wrap around motion. Therefore, the knee joint is primarily subjected to combined load from shearing and bending. Since the EEVC legform uses pure shear displacement as a measure for ACL failure, the lack of the contribution from bending motion to the ACL failure measure used (shear displacement) would result in poor

correlation from the human model ACL elongation, as opposed to the FlexGTR that employs the ACL elongation. In contrast, much better correlation between the EEVC legform model knee bending angle and the human model MCL elongation suggests that the elongation of the MCL is primarily determined by the knee bending and the contribution from the knee shear is not significant.

In the further investigation of the factors for the difference in the tibia fracture measure correlation, it was found that the trend of the change of the peak injury measures at BP height when SP location was varied (left two bar charts in Figure 17) was totally different between the bending moment and the acceleration. Figure 19 shows the time histories of the total load applied from BP and SP for Bone and Steel tibia stiffness levels and the vehicle models V3, V4 and V5. The time history plots show that the total applied load increased as SP moved forward from V3 to V5. The results of the simplified tibia impact simulations clarified that the tibia acceleration is solely determined by the magnitude of the applied load, while the tibia bending moment is affected by both the magnitude and the location of the applied load (see Figure 18). This finding can also be confirmed by the theoretical study done by Mizuno et al. [15]. This difference in the determinants of different tibia fracture measures explains the reason why the trend was totally different between the bending moment and the acceleration as shown in Figure 17. Since the acceleration is determined solely by the magnitude of the applied load, it increased as SP moved forward due to increased peak applied load. In contrast, since the bending moment depends on both the magnitude and the location of the applied load, the reason for the slight decrease of the bending moment as SP moves forward would be that the contribution of the effective loading location due to the difference in the horizontal location of SP was larger than that of the magnitude of the total applied load in the loading environment provided by the vehicle model used. This could also explain why a negative correlation was seen between the EEVC legform model upper tibia acceleration and the human model tibia bending moment in the correlation analysis. Based on these results, it is suggested that the use of the tibia bending moment as a tibia fracture measure and the bending stiffness of the bony structure of the legform close to that of the human leg leads to better prevention measures of pedestrian tibia fracture.

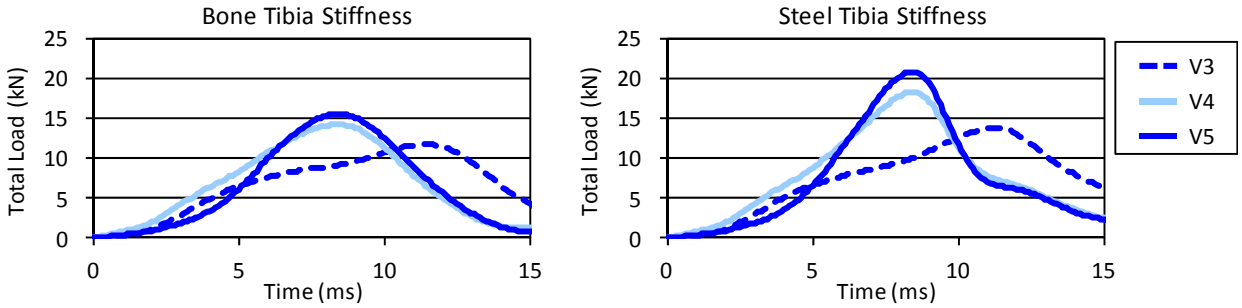

Fig. 19. Time histories of total load applied from BP and SP for Bone and Steel tibia stiffness levels and vehicle models V3, V4 and V5

Since all the results described in the paper were obtained from FE simulations using the human FE model and the FE models of the legforms, the validity of the results depends on the model validation described in this paper.

V. CONCLUSIONS

In a lateral impact from a vehicle to a pedestrian simulated using the human FE model, the peak tibia von Mises stress correlated well with the tibia bending moment at the time of the peak von Mises stress, while the tibia acceleration at the time of the peak von Mises stress showed a poor correlation. The correlation of the peak injury measures from the impact simulations using FE models of a human body, FlexGTR and EEVC legform was found to be significantly improved with the FlexGTR relative to the EEVC legform for the tibia fracture and ACL failure measures. The results of the impact simulations using the EEVC legform FE model with the bone stiffness varied showed that the excessive stiffness of the tibia relative to a human generally resulted in higher sensitivity to the difference in the stiffness and geometric characteristics. It also yielded an exceptionally high acceleration response in some combinations of the vehicle stiffness and geometric characteristics. Simplified tibia impact simulations showed that both the tibia bending moment and the tibia acceleration were found to be equally sensitive to the magnitude of the applied load, while only the tibia bending moment showed

sensitivity to the loading location relative to the center of gravity of the tibia. Due to this difference, the tibia bending moment and the tibia acceleration of the legform showed a significantly different trend when the horizontal location of the lower part of the bumper was changed.

VI. REFERENCES

[1] International Road Traffic and Accident Database, "IRTAD Database, July 2011 -- Fatalities by road use" Internet: http://internationaltransportforum.org/irtadpublic/pdf/roaduse.pdf, 2011.

[2] Institute for Traffic Accident Research and Data Analysis, "2010 Traffic Accident Statistics" (in Japanese), 2011.

[3] National Highway Traffic Safety Administration, "National Automotive Sampling System, Pedestrian Crash Data Study", 1994-1998.

[4] "Global technical regulation No. 9 (gtr 9) : PEDESTRIAN SAFETY (Established in the Global Registry on 12 November 2008)", ECE/TRANS/180/Add.9, 2009.

[5] Konosu A, Issiki T, Takahashi Y, Suzuki H, Been B, Burleigh M, Hirasawa T, Kanoshima H, Development of a Biofidelic Flexible Pedestrian Legform Impactor Type GTR Prototype Part 1: Development and Technical Evaluations, *Proceedings of 21st ESV Conference*, Stuttgart, Germany, Paper Number 09-0145, 2009.

[6] Matsui Y, Biofidelity of TRL Legform Impactor and Injury Tolerance of the Human Leg in Lateral Impact, *Stapp Car Crash Journal*, Vol. 45, 2001.

[7] Konosu A, Issiki T, Takahashi Y, Evaluation of the Validity of the Tibia Fracture Assessment using the Upper Tibia Acceleration Employed in the TRL Legform Impactor, *Proceedings of IRCOBI Conference*, 2009.

[8] Konosu A, Issiki T, Tanahashi M, Suzuki H, Development of a Flexible Pedestrian Legform Impactor Type GT (Flex-GT), *Proceedings of 20th ESV Conference*, Lyon, France, Paper Number 07-0178, 2007.

[9] Japan Automobile Manufacturers Association and Japan Automobile Research Institute, Development of a FE Flex-GTR-prototype Model and Analysis of the Correlation between the Flex-GTR-prototype and Human Lower Limb Outputs using Computer Simulation Models, 8th Flex-TEG Meeting Document, Number TEG-096, 2009.

[10] Takahashi Y, Suzuki S, Ikeda M, Gunji Y, Investigation on Pedestrian Pelvis Loading Mechanisms Using Finite Element Simulations, *IRCOBI Conference*, Hannover, Germany, 2010.

[11] Ikeda M, Suzuki S, Gunji Y, Takahashi Y, Motozawa Y, Hitosugi M, Development of An Advanced Finite Element Model for a Pedestrian Pelvis, *Proceedings of 22nd ESV Conference*, Washington DC, USA, Paper Number 11-0009, 2011.

[12] Japan Automobile Manufacturers Association and Japan Automobile Research Institute, Flex-GT Full Calibration Test Procedures, 5th Flex-TEG Meeting Document, Number TEG-047, 2007.

[13] "Global technical regulation No. 9 (Pedestrian Safety) – Phase-2 of the global technical regulation, Proposal for Amendment 2 ", ECE/TRANS/WP.29/GRSP/2011/13, 2011.

[14] Takahashi Y, Suzuki S, Okamoto M, Oda S, Fredriksson R, Pipkorn B, Effect of Stiffness Characteristics of Vehicle Front-end Structures on Pedestrian Pelvis and Lower Limb Injury Measures, *IRCOBI Conference*, Krakow, Poland, 2011.

[15] Mizuno K, Ueyama T, Nakane D, Wanami S, Comparison of Reponses of the Flex-PLI and TRL Legform Impactors in Pedestrian Tests, *SAE World Congress*, Detroit, USA, Paper Number 2012-01-0270, 2012.